Processing and tribological behaviour of carbon fiber reinforced polylactic acid composites

Processing and tribological behaviour of carbon fiber reinforced polylactic acid composites

B. Suresha[1]*, Vikas Hanamasagar[1] and A. Anand[1]

[1]Department of Mechanical Engineering, The National Institute of Engineering, Mysuru-570 008, India

*Corresponding Author: B. Suresha, sureshab@nie.ac.in

ABSTRACT

Thermoplastic composites are acquiring more importance in various tribological applications due to their self-lubricity, low melting, and ease of fabrication. In this research article, processing via fused deposition modelling and dry sliding wear behaviour of neat and short carbon fiber reinforced polylactic acid composites have been investigated. A series of wear tests using a pin-on-disc wear apparatus was carried out by varying tribo-parameters namely applied load (10, 20, and 30 N), sliding velocity (0.5, 1.0, and 1.5 m/s), and sliding distance (1000, 2000, and 3000 m) following the response surface methodology. Analysis of variance was performed for optimizing the operating parameters with respect to minimum specific wear rate. The experimental outcomes showed decrease in specific wear rate of polylactic acid composites by 70 % in comparison to neat polylactic acid, due to reinforcement of short carbon fibers. Worn surface morphology of neat polylactic acid and carbon fiber reinforced polylactic acid show fine groves in the sliding direction, thinning of fibers and net work of microcracks and few pull-out of fibres from the matrix material.

Keywords: Short carbon fiber reinforced polylactic acid; Response surface methodology; Dry sliding wear; Analysis of variance; Worn surface morphology

1 INTRODUCTION

Thermoplastics belong to a group of polymers that are acquiring a lot of interest due to their ability to soften and melt by the application of heat and can be processed easily either in liquid or heat softened state making them reusable. Thermoplastics are being employed in many different applications due to its ability to improve the desired mechanical and thermal characteristics by suitable addition of reinforcements. The most used manufacturing processes for fabrication of thermoplastics are thermoforming, extrusion, blow moulding, injection moulding and many more [1]. Among the various thermoplastics, polylactic acid (PLA) based thermoplastics are being widely employed in automotive and aerospace applications such as, sliders, bearings, cams and gears because of their better mechanical and thermal properties [2]. Additive manufacturing (AM) has been recently developed as a rapid prototyping technique with its ability to develop complex designed structures with minimum material waste, low cost and higher accuracy as compared with other conventional methods [3].

Due to excessive demand from industries, a wide variety of 3D printing technologies have been developed such as selective laser sintering (SLS), stereo lithography, selective laser melting (SLM) and fused deposition modelling (FDM) [4]. Fused deposition modelling is an AM technique wherein raw

material in filament form is passed through the rollers and the heating unit assists in melting of filament, that is layered on to the build platform as per required dimensions and this process continues until the desired structure is obtained [05]. Tymrak et al., [6] found that printing parameters have notable influence on the mechanical characteristics of FDM fabricated parts. The results show that the average tensile strength of acrylonitrile butadiene styrene and PLA specimens are 29 MPa and 57 MPa respectively. Addition of fibers/fillers is the most convenient way to enhance the mechanical, tribological and thermal characteristics of composites [7]. Lopes et al., Wang et al., and Sonsalla et al., [8-10] confirmed that reinforcing of ABS and PLA composites with carbon fibers resulted in improvement of both mechanical and thermal properties. Aqzna et al., [11] investigations showed an improvement in Young's modulus, impact strength, and Rockwell hardness by 21%, 18% and 93% respectively by the addition of zinc ferrite nanoparticles as compared to neat ABS polymer.

Friction, wear and fatigue are the most typically encountered problems in industries resulting in engineering part damage and replacements [12]. Recently, the attention of research is being focussed on study of tribological behaviour of thermoplastics fabricated by AM method. Abdualla et al., [13] studied the results due to different infill geometries on tribological behaviour of ABS specimens fabricated by FDM technique using Pin-on-disc apparatus. Results indicated that the coefficient of friction (CoF) value ranged from 0.27 to 0.51 and wear rate ranged from 0.27×10^{-6} to 0.24×10^{-6} mm^3/Nm. It was noted that both solid and triangular infill pattern showed lower CoF and specific wear rate in comparison to other infill geometries. Sahar et al., [14] looked into the impact of layer orientation and layer thickness on wear and friction properties of PLA samples. Analysis of variance findings proved the influence of layer thickness was insignificant in comparison to normal load and build orientation. The worn surface morphology studies revealed adhesive wear was more dominant as compared to fatigue wear. Kumar et al., [15] illustrated that specific wear rate of ABS specimens raised as the applied load and sliding velocity increased, whereas CoF reduces with higher sliding velocity and sliding distance. Pawlak et al., [16] compared the friction characteristics of PLA fabricated by injection moulding and FDM technique. The results revealed that CoF of specimen fabricated with FDM and injection moulding were similar in the range of 0.35 to 0.55. Pramendra et al., [17] showed that specific wear rate and CoF of PLA composites can be reduced significantly by using natural fibers as reinforcements. Response surface methodology (RSM) serves as a good statistical tool for analysis and optimization of responses efficiently with minimum number of trials [18].

From the literature review, addition of short carbon fibers into various thermoplastic polymers had shown considerable improvement in mechanical, thermal and tribological properties fabricated by conventional methods namely compression moulding, extrusion, injection moulding and so on. The present article focusses on the effect of short carbon fiber reinforcement on dry sliding wear behaviour of PLA composites fabricated by FDM technique.

2 MATERIALS AND METHODS

Materials

Filaments namely Polylactic acid (PLA) and 20 wt. % short carbon fiber reinforced polylactic acid (CF-PLA) composites having 1.75 mm fiber diameter were purchased from eSUN 3D, Karnataka, India. The fiber loading of 20 wt. % in PLA was limited due to optimum strength and stiffness of the final composites by 3D printing. Furthermore, the 20-wt. % carbon fiber reinforcement is found to be optimum for better interfacial bonding between the fiber and matrix, and addition of carbon fiber > 20 wt. % makes the filament brittle and not favourable to produce composites by 3D printing. Table 1 represents the physical and mechanical properties of PLA and CF-PLA composite.

Table 1. Physical and mechanical properties of PLA and CF-PLA composites

Parameters	PLA	CF-PLA
Melting point (^{o}C)	195 – 215	215-225
Glass transition (^{o}C)	60 – 65	60-70
Density (g/cm^{3})	1.21-1.43	1.29 -1.5
Tensile strength (MPa)	48	59
Flexural strength (MPa)	89	106

Fabrication of PLA and CF-PLA composites

Figure 1 represents the process flow chart for preparation of PLA and CF-PLA composites using FDM technique. The first step is preparation of the CAD model of required samples using mechanical modelling software's, which is than sliced using an Ultimaker Cura slicing software for development of G-codes. The process parameters considered for printing of samples is as shown in table 2.2.1. The G codes developed are provided as an input for Creality Ender-3 Pro FDM printer. The material in the form of filament is supplied through the rollers to the heating unit, which is heated to a pre-determined temperature at the nozzle and then moved according to the G-codes, depositing the material on the build platform. This procedure is repeated until required samples are obtained and are removed after cooling of samples.

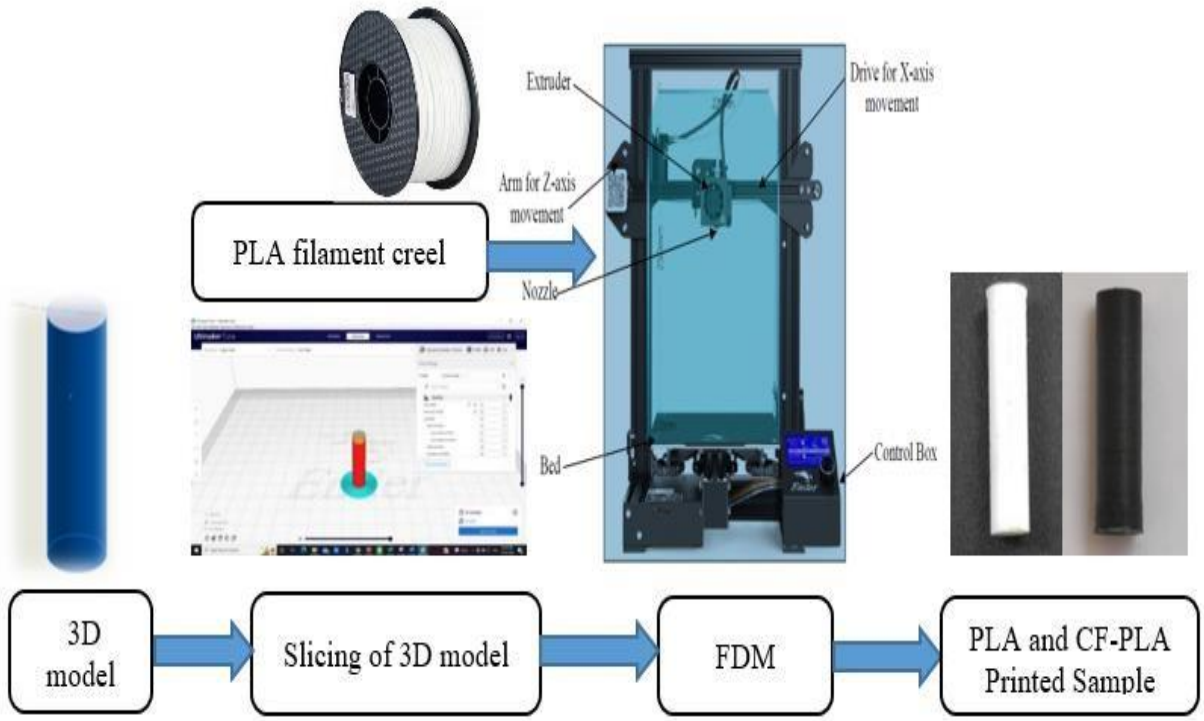

Figure 1. Process flow chart of PLA and CF-PLA composites using FDM

Table 2. Printing parameters for fabrication of PLA and CF-PLA composite

Material / Parameters	PLA	CF-PLA
Nozzle Temperature (^{0}C)	205	210
Bed Temperature (^{0}C)	60	60
Layer thickness(mm)	0.12	0.12
Infill Density (%)	100	100
Printing Speed (mm/sec)	70	70
Build Orientation	Vertical	Vertical
Infill Pattern	Lines	Lines

Density measurement

Density of neat PLA and CF-PLA composite samples was measured using high precision electronic weighing machine following Archimedes' principle as per ASTM D792 standards [19]. The mass of sample in air was recorded and mass of sample submerged in distilled water at room temperature was noted. Based on equation (1), the sample density was determined experimentally. The theoretical density of samples was determined by rule of mixtures using equation (2).

$$\rho_{ex} = \frac{M_a}{M_a - M_w} S \quad (1)$$

where, ρ_{ex} is measured density of sample (g/cm^3), M_a is the mass of sample in air (g), M_w is the mass of sample in distilled water (g), and S= specific gravity of water (g/cm^3).

$$\frac{1}{\rho_{th}} = \frac{M_m}{\rho_m} + \frac{M_r}{\rho_r} \quad (2)$$

where, ρ_{th} is theoretical density of sample (g/cm^3), M_m is the mass fraction of matrix (g), M_r is mass fraction of reinforcement (g), $\rho_m$is the density of matrix (g/cm^3) and ρ_r is the density of reinforcement (g/cm^3).

Dry sliding wear test

Dry sliding wear experiments were conducted using Pin-on-disc apparatus following ASTM G99 standards [20]. The Pin-on-disc apparatus is as viewed in Figure 2. The cylindrical samples of length 30 mm and 8 mm diameter was used for conducting the wear test. The track diameter of 70 mm was maintained for conduction of all experiments. Before the test, the sample and the counter face were cleaned with acetone for removal of debris. The mass of sample before test and after test are measured to determine the wear volume of samples using equation (3).

$$V_w = \frac{m_i - m_f}{\rho_{ex}} \quad (3)$$

where, V_w represents wear volume (mm^3), m_i is the initial mass of sample (g), m_f is the final mass of sample (g), ρ_{ex} represents measured density of the sample (g cm^{-3}). Further, the specific wear rate (K_s) is determined using equation (4).

$$K_S = \frac{V_w}{P \times D} \quad (4)$$

where, K_S represents specific wear rate (mm^3/ N-m), V_w is the wear volume (mm^3), P is the applied normal load (N), and D is the sliding distance (m).

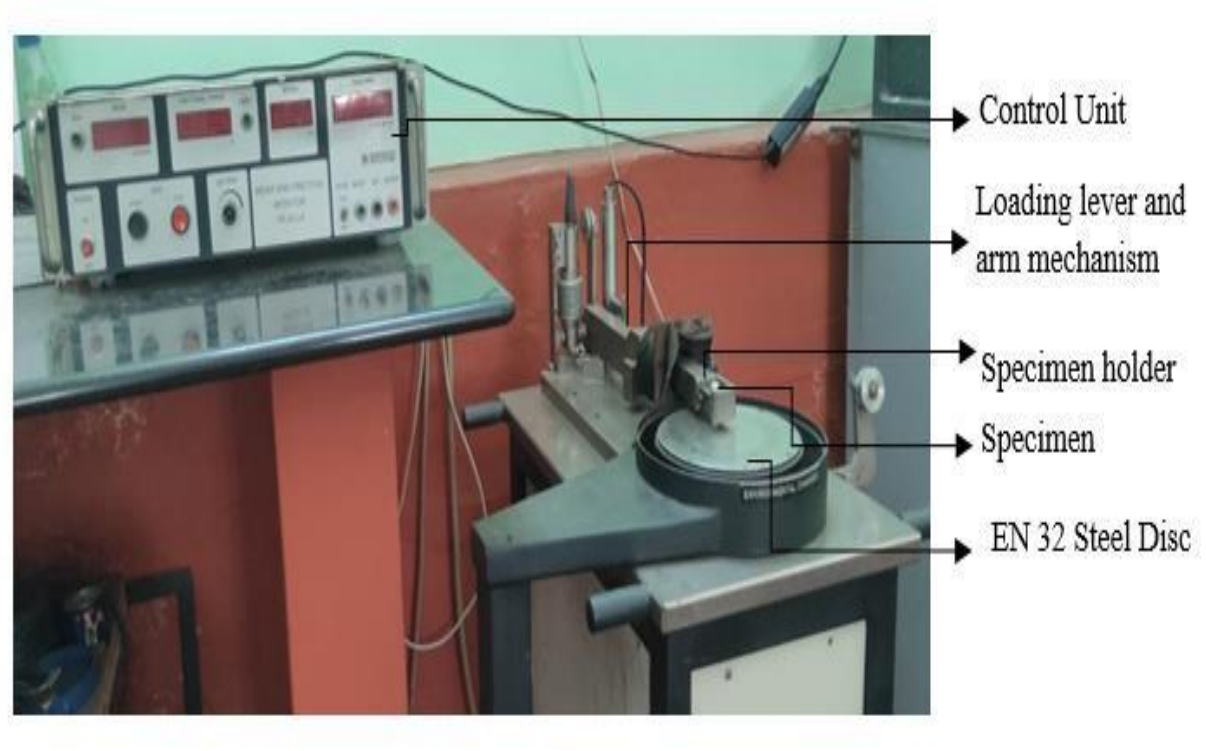

Figure 2. Pin on disc apparatus

In this present experimental work, the input tribo-parameters such as applied load, sliding velocity and sliding distance were modelled and optimised using Box-Behnken design via Response surface methodology (RSM) for minimizing number of trails and time in finding minimum K_S as response parameter. Minitab 19.1, a statistical software was used for creating and analysing of design matrix. Table 3 summarizes the factors and their levels considered for experimental design.

Table 3. Factors and their levels considered in Box Behnken Design

Control factors	Designation	Levels		
		Low (-1)	Medium (0)	High (+1)
Applied load (N)	A	10	20	30
Sliding velocity(m/s)	B	0.5	1.0	1.5
Sliding distance(m)	C	1000	2000	3000

3 RESULTS AND DISCUSSION

Effect of carbon fiber on density of PLA composite

The results of measured density for PLA and CF-PLA composites are listed in Table 4. The difference between experimental and theoretical densities indicate presence of voids and pores in the fabricated composite samples, that have a considerable impact on the material properties [17]. The CF-PLA

samples showed increase in density with comparison to PLA samples, this is because the carbon fibers possess high density and good adhesion with PLA matrix thereby resulting in increased density as compared to PLA. The decreased void percent reported for PLA and CF-PLA samples was owing to strong interlayer bonding obtained between layers of samples with less air gaps, confirming the efficiency of the FDM process used for composite fabrication.

Table 4. Measured density of PLA and CF-PLA composites

Sl. No	Material	Theoretical Density (g cm^{-3})	Experimental Density (g cm^{-3})	Voids (%)
1.	PLA	1.23	1.20	2.44
2.	CF-PLA	1.26	1.22	3.18

Effect of carbon fibers on K_S of PLA composite

Table 5 presents the experimental design obtained by Box-Behnken design and the experimental outcomes and the Specific wear rate (K_S) obtained for PLA and CF-PLA composite. The experiments were performed as per design and the K_S values were determined. The minimum *Ks* value for PLA composites obtained was 0.0931under applied load of 10 N, sliding velocity of 1 m/s and 1000 m sliding distance, whereas the Ks value for CF-PLA composites was 0.0707 at the same wear test conditions.

Table 5. Experimental design and results of composites

Sl. No.	Load (N)	Velocity (m/s)	Distance (m)	*Ks* (10^{-13} mm^3/N m)	
				PLA	CF-PLA
01	10	0.5	2000	0.2014	0.1017
02	30	0.5	2000	0.9652	0.9154
03	10	1.5	2000	0.2115	0.1515
04	30	1.5	2000	1.2500	1.2514
05	10	1.0	1000	0.0931	0.0707
06	30	1.0	1000	0.6525	0.6535
07	10	1.0	3000	0.3317	0.1371
08	30	1.0	3000	1.5021	1.5012
09	20	0.5	1000	0.8012	0.7501
10	20	1.5	1000	1.0100	0.9317
11	20	0.5	3000	1.0512	0.9615
12	20	1.5	3000	1.4012	1.3512
13	20	1.0	2000	1.0221	0.9514
14	20	1.0	2000	1.1125	0.9914
15	20	1.0	2000	1.1254	0.9774

The statistical approach of Analysis of variance (ANOVA) was used to generate a set of conclusions according to the experimental results and significant contributions of each factor on the response [21]. ANOVA was performed for 5% level of significance and 95% degree of confidence. Tables 6 and 7 list the results of the ANOVA test for K_S of PLA and CF-PLA composites respectively.

Table 6. ANOVA results of *Ks* for PLA composite

Source	DF	Adj SS	Adj MS	F-Value	P-Value	Contribution (%)
Linear	3	2.1044	0.7014	74.31	0	71.3766
A	1	1.6129	1.6129	170.88	0	54.7101
B	1	0.0911	0.0911	9.65	0.027	3.0901
C	1	0.4002	0.4002	42.41	0.001	13.5762
Square	3	0.6968	0.2323	24.61	0.002	23.6387
A×A	1	0.6917	0.6917	73.29	0	23.4651
B×B	1	0.000	0.0000	0	0.952	0.00135
C×C	1	0.0021	0.0021	0.22	0.655	0.0719

R-sq=98.40%, R-sq(adj)= 95.52%, R-sq (pred)= 77.34%

Table 7. ANOVA results for *Ks* of CF-PLA composite

Source	DF	Adj SS	Adj MS	F-Value	P-Value	Contribution (%)
Linear	3	2.2758	0.7586	248.09	0	74.75504
A	1	1.8629	1.8629	609.23	0	61.19263
B	1	0.1145	0.1145	37.45	0.002	3.761369
C	1	0.2983	0.2983	97.58	0	9.801043
Square	3	0.5693	0.1897	62.06	0	18.70173
A×A	1	0.5564	0.5564	181.97	0	18.27734
B\×B	1	0.0014	0.0014	0.47	0.522	0.047629
C×C	1	0.0001	0.0001	0.04	0.858	0.003613

R-sq=99.5%, R-sq(adj)= 98.59%, R-sq (pred)= 92.34%

It is clear from the ANOVA results that applied load has the highest significant contribution of 54.71% and 61.19% on *Ks* of PLA and CF-PLA composites respectively, followed by sliding distance (13.97% and 9.80%) and sliding velocity (3.09% and 3.76%). The R-square values obtained are nearer to 100% which states that the experimental models are more valid and in good correlation to experimental data. The higher values of R-square (adj) and R-square (pred) resembles good predictability of model. The normal probability plots of *Ks* are as depicted in figure 3, wherein the residuals are approaching towards straight line indicating that the experimental results obtained are normally distributed and dependable. The quadratic regression models obtained with respect to *Ks* of PLA and CF-PLA samples are shown in equations 5 and 6 respectively. The K_S values obtained by experimentation were compared with the K_S values obtained by regression models and were closer within acceptable error.

$$Ks = -1.320 + 0.176 \times A - 0.228 \times B - 0.000027 \times C - 0.004328 \times A^2 + 0.013 \times B^2 + 0.000054 \times C^2 + 0.01374 \times A \times B + 0.000014 \times A \times C + 0.000071 \times B \times C \quad (5)$$

$$Ks = -0.794 + 0.1502 \times A - 0.414 \times B - 0.000323 \times C - 0.003882 \times A^2 + 0.079 \times B^2 + 0.00032 \times C^2 + 0.01431 \times A \times B + 0.000020 \times A \times C + 0.000104 \times B \times C \quad (6)$$

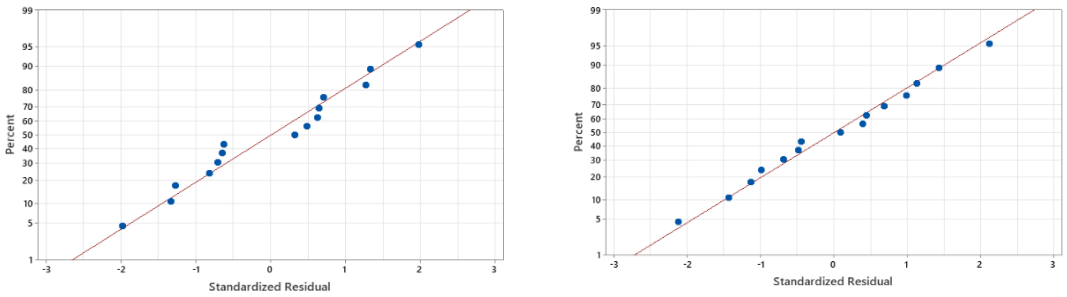

(a) (b)

Figure 3. Normal probability plot for *Ks* of (a) PLA (b) CF-PLA

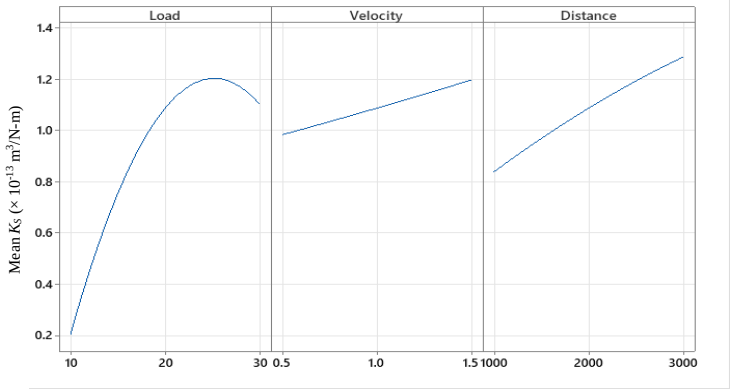

Figure 4. Effect of control factors on K_S of PLA

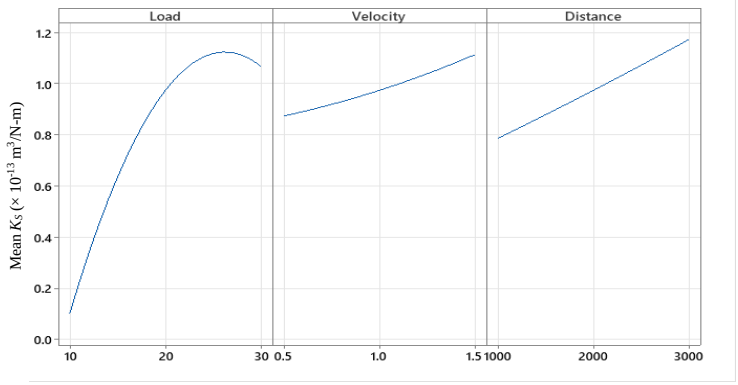

Figure 5. Effect of control factors on K_S of CF-PLA

Figures 4 and 5 represent the plots for effect of control factors on the K_S of PLA and CF-PLA composites respectively. It is noted that as the applied load increased from 10 N to 20 N, there was an increment in mean *Ks* up to 1.1 mm^3/Nm for CF-PLA composites, which was less as compared to PLA composites. PLA composites have poor wear performance due to the process of softening, as well as formation of layered film on counter face during sliding [22]. With increase in load applied, the stress developed at the interface increases, resulting plastic deformation of the sample and increase in *Ks* trends. Increase in sliding velocity from 0.5 m/s to 1.5 m/s caused the counter face to deliver more shearing action to the sample surface, resulting in increased material removal, the obtained trends are in line with previous literature works [14-16]. The *Ks* value at maximum sliding velocity for CF-PLA

composite was lower as compared to PLA composites due to improvement in shear strength of PLA composite by presence of carbon fibers.

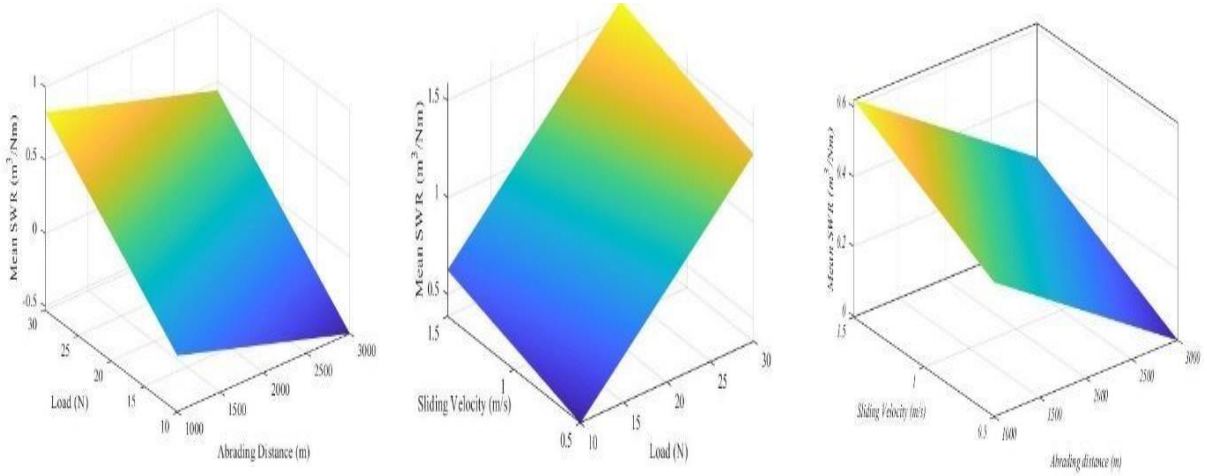

(a) (b) (c)

Figure 6. Surface plots of *Ks* for (a) load vs distance, (b) velocity vs load, (c) velocity vs distance

Figure 6 represents the surface plots obtained for different interactions between applied load, sliding distance and sliding velocity. It is noted that with increase in sliding velocity at lower load, the K_S value tend to increased significantly. The plot of applied load vs sliding distance in Figure 5c demonstrates that at lower load, with increase in the sliding distance, the K_S value increased drastically.

Optimisation of K_S

Response surface methodology desirability optimization analyses experimental results and predicts the best independent factors along with corresponding levels and responses. A number of iterations were carried out to obtain the optimize value with respect to minimum *Ks*. Figure 7 represents the optimization plot showing the optimum wear conditions for independent factors of load applied, sliding velocity and sliding distance for PLA and CF-PLA composites respectively. To verify the repeatability and reliability of the predicted optimum wear conditions, an experimental test was carried out. Table 8 represents the predicted and experimental results obtained at the optimum wear conditions with respect to minimum *Ks* for PLA and CF-PLA samples. The *Ks* value obtained by confirmation experiment are closer to the experimental *Ks* value obtained by RSM. The K_S value obtained experimentally for CF-PLA composite at optimised condition was lower in comparison to PLA composite. K_S value of PLA composite was reduced due to higher load bearing capacity along with increased strength and stiffness by reinforcement of carbon fibers, the obtained results are in line with the previous literature works [12-23].

Table 8. Confirmation experiments for *Ks*

Material	Applied load (N)	Sliding velocity (m/s)	Sliding Distance (m)	Predicted *Ks* (10^{-13}m^3/Nm)	Experimental *Ks* (10^{-13}m^3/Nm)	Error (%)
PLA	10	0.78	1000	0.0943	0.0901	4.45
CF-PLA	10	0.5	3000	0.0255	0.0270	5.55

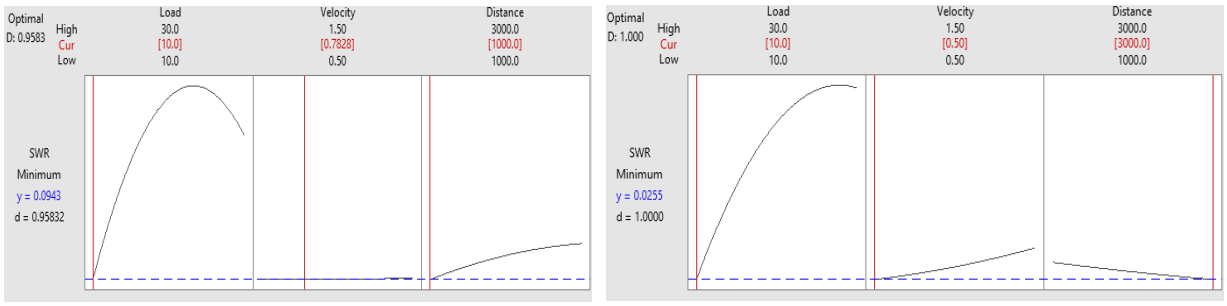

(a) (b)

Figure 7. Desirability plot for minimum K_S of PLA and CF-PLA composite

(a) (b)

Figure 8. Samples for PLA and CF-PLA composite (a) Before test, (b) After test

Worn surface morphology

The optical images as represented in figure 8 indicate the deformation characteristics of worn samples. The samples are subjected to shear stress and the material at the surface of sample is deformed along the tangential component of sliding direction. This wear type is formed due to localised bonding developed between the surface of sample and the counter disc surface as a result of increase in temperature at the interface. The wear debris from the worn-out samples was adhered to the counter face forming a thin transfer layer [14] as shown in Figure 9.

The features of worn surface of PLA and CF-PLA composites for 30 N applied load and sliding distance of 3000 m are as depicted in Figures 10 and 11. As observed from Figure 10, the depth of grooves is steeper at higher load, which indicates higher wear loss of neat PLA sample. Similar observations were obtained during experimentation at higher load and sliding distance.

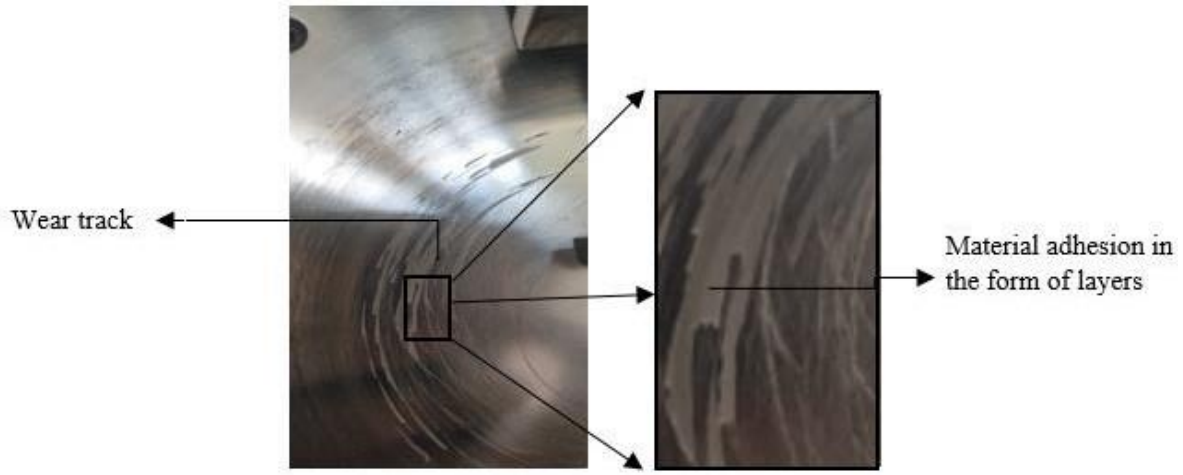

Figure 9. Surface image of counter face after wear test of composite

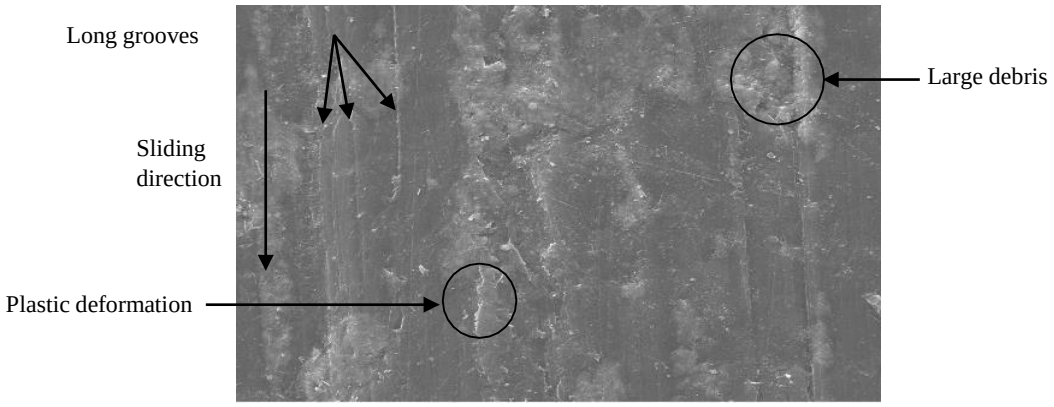

Figure 10. Worn surface features of PLA composites

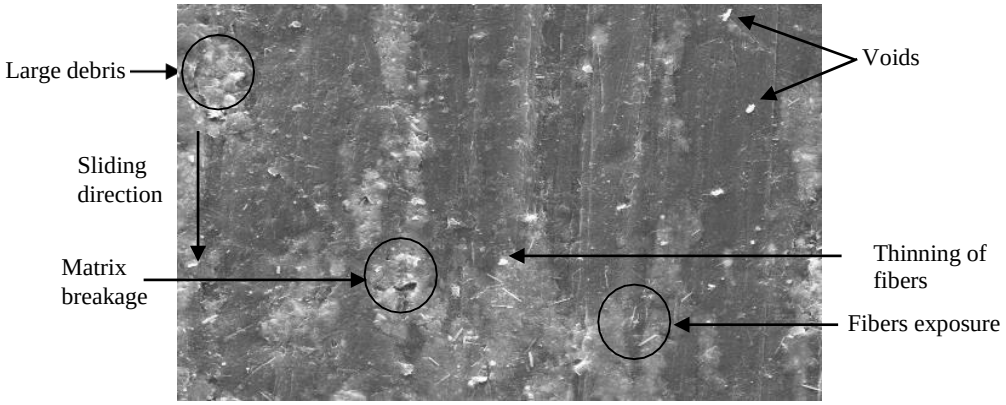

Figure 11. Worn surface features of CF-PLA composites

Figure 11 shows the exposure of carbon fibers in the matrix, thinning of fibers in the sliding direction and few fibers pull-out. The carbon fibers embedded in the matrix assist in providing support and protect the matrix from being worn during sliding, hence reducing wear loss. There was no detachment or pull

out of fibers observed, replicating high strength and load bearing ability of carbon fibers. Accumulation of debris and formation of transfer film can be observed representing adhesive wear as the predominant wear mechanism.

4 CONCLUSION

The composite samples were fabricated successfully by using Fused deposition modelling technique. The effect of short carbon fibers on density and tribological behaviour on PLA-based thermoplastics were investigated. The inclusion of carbon fibers increased the density of PLA samples by 1.3 percent, owing to the higher density of carbon fibers and efficiency of FDM technique. The ANOVA findings disclosed that load applied had a substantial effect on minimization of K_S followed by sliding distance and sliding velocity. The RSM method projected the best outcomes for the combination of all independent factors, resulting in the lower specific wear rate. The optimum results obtained by statistical approach were validated by conducting a confirmation test and the obtained results were in concurrencewith experimental outcomes. By incorporation of carbon fibers, the specific wear rate was reduced by 70% in comparison to neat PLA samples. This reduction was attributed to the inclusion of carbon fibers improving the lubricating property and stiffness of PLA composite. The SEM micrographs of worn surfaces of PLA and CF-PLA samples showed adhesive wear as the primary wear mechanism.

REFERENCES

[1] Biron M., (2018). *Thermoplastics and thermoplastic composites*, William Andrew, Elsevier.

[2] Andrew J.J and Dhakal H.N., (2022). Sustainable bio based composites for advanced applications: recent trends and future opportunities–A critical review, *Composites Part C: Open Access,* Vol. 7, pp.100-220.

[3] Mueller B., (2012). Additive manufacturing technologies –Rapid prototyping to direct digital manufacturing. *Assembly Automation*, Vol. 32, Emerald Group Publishing Limited.

[4] Gibson I, Rosen D.W, Stucker B, Khorasani M, Rosen D, Stucker B, Khorasani M., (2021). *Additive manufacturing technologies*, Vol. 17, Cham, Switzerland: Springer.

[5] Pavan Kumar Penumakala, Jose Santo, Alen Thomas., (2020). A critical review on the fused deposition modelling of thermoplastic polymer composites, *Composites: Part B*, Vol. 201, pp. 108336.

[6] Tymrak B.M, Kreiger M, Pearce J.M., (2014). Mechanical properties of components fabricated with open-source 3-D printers under realistic environmental conditions. *Materials & Design*, Vol. 58, pp. 242-246.

[7] Sajjad Mamaghani Shishavan, Taher Azdast, Samrand Rash Ahmadi., (2014). Investigation of the effect of nano clay and processing parameters on the tensile strength and hardness of injection molded Acrylonitrile Butadiene Styrene–organoclay nanocomposites. *Materials and Design,* Vol. 58, pp527-534.

[8] Lopes B.J. and Almeida D., (2019). Initial development and characterization of carbon fiber reinforced ABS for future Additive Manufacturing applications. *Materials Today: Proceedings*, Vol. 8, pp.719-730.

[9] Wang Kui, Li Shixan, Rao Yanni, Yiyun Wu, Peng Yong, Yao Song, Honghao Zhang, Said Ahzi.,(2019). Flexure behaviours of ABS-based composites containing carbon and Kevlar fibers by material extrusion 3D printing. *Polymers*, Vol. 11, pp.1878.

[10] Sonsalla T, Moore A.L, Meng W.J, Radadia A.D, Weiss L., (2018). 3-D printer settingseffects on the thermal conductivity of acrylonitrile butadiene styrene (ABS). *Polymer Testing*, Vol. 70, pp.389-395.

[11] Aqzna S.S, Yeoh C.K, Idris M.S, Teh P.L, Bin Hamzah K.A, Atiqah T.N., (2018). Effect of different filler content of ABS–zinc ferrite composites on mechanical, electrical and thermal conductivity by using 3D printing. *Journal of Vinyl and Additive Technology*, Vol. 24, pp. E217-E229.

[12] Shrinivasan R, Suresh Babu, Udhaya Rani V, Suganthi M, Dheenasagar R., (2020). Comparison of tribological behaviour for parts fabricated through fused deposition modelling process on ABS and 20% carbon fibre PLA, *Materials today: Proceedings*, Vol. 27, pp. 1780-1786.
[13] Abdollah M.F.B, Norani M.N.M, Abdullah M.I.H.C, Amiruddin H, Ramli F.R, Tamaldin N., (2020). Synergistic effect of loads and speeds on the dry sliding behaviour of fused filament fabrication 3D-printed acrylonitrile butadiene styrene pins with different internal geometries, *The International Journal of Advanced Manufacturing Technology*, Vol. 108, pp.2525- 2539.
[14] Sahar Zhiani Hervan, Atakan Altın kaynak, Zeynep Parlar., (2020), Hardness, friction and wear characteristics of 3D-printed PLA polymer, Proc. I, Part J: *Journal of Engineering Tribology.* Vol. 235, pp.1590-1598.
[15] Kumar S. and Roy B.S., (2020). Tribological properties of acrylonitrile butadiene styrene in self–mated contacts and against steel disc. *Materials Today: Proceedings*, Vol. 26, pp.2388-2394.
[16] Pawlak W, Wieleba W, Wroblewsk R., (2019). Research of tribological properties of polylactide (PLA) in the 3D printing process in comparison to the injection process. *Tribologia.* Vol. 1, pp. 25-28.
[17] Pramendra Kumar Bajpai, Inderdeep Singh, Jitendra Madaan., (2013). Tribological behaviour of natural fiber reinforced PLA composites, *Wear,* Vol. 297, pp. 829-840.
[18] Abhijeet Nayak, Dipak Kumar Jesthi, Bharat Chandra Routara, Diptikanta Das, Ramesh Kumar Nayak., (2018). Tribological properties of glass/carbon hybrid composites through inter-ply arrangement using Response Surface Methodology. *Materials Today: Proceedings,* Vol. 5, pp. 19828- 19835.
[19] ASTM D792-20., (2020). *Standard Test Methods for Density and Specific Gravity (Relative Density) of Plastics by Displacement*, West Conshohocken, ASTM International.
[20] ASTM G99-17., (2017). *Standard Test Method for Wear Testing with a Pin-on-Disk Apparatus*, West Conshohocken, ASTM International.
[21] Divya G.S, Suresha B, Somashekar M, Jamadar I.M., (2021). Dynamic Mechanical Analysis and Optimization of Hybrid Carbon-Epoxy Composites Wear Using Taguchi Method, *Tribology in industry*, Vol 43, pp. 298-309.
[22] Ziyan Man, Hongjian Wang, Qinghao He, Dae-Eun Kim, Li Chang., (2021). Friction and wear behaviour of additively manufactured continuous carbon fibre reinforced PA6 composites. *Composites: Part B*, Vol. 226. Pp. 109332.
[23] Sudin M. N, Ramli F. R, Alkahari M. R, Abdullah M. A., (2018). Comparison of wear behaviour of ABS and ABS composite parts fabricated via fused deposition modelling, *International Journal of Advanced and Applied Sciences*, Vol. 5, pp. 164-169.